Available online at www.sciencedirect.com
ScienceDirect
Journal of Catalysis 242 (2006) 254–269
JOURNAL OF CATALYSIS
www.elsevier.com/locate/jcat

Effect of Ti on the catalytic properties of CoMo/Ti(x)-HMS catalysts in the reaction of hydrodesulfurization of 4-ethyl-6-methyl dibenzothiophene

T.A. Zepeda [a], B. Pawelec [b], J.L.G. Fierro [b], T. Halachev [a,*]

[a] *Centro de Física Aplicada y Tecnología Avanzada, Universidad Nacional Autónoma de México, A.P. 1-1010, Querétaro, Qro. 76000, Mexico*
[b] *Instituto de Catálisis y Petroleoquímica, CSIC, c/Marie Curie 2, Cantoblanco, 28049 Madrid, Spain* [1]

Received 14 January 2006; revised 8 June 2006; accepted 11 June 2006

Available online 17 July 2006

Abstract

The effect of the presence of varying titanium concentrations introduced into hexagonal mesoporous silica (HMS) support on the catalytic activity of the catalysts was evaluated in the hydrodesulfurization of 4-ethyl-6-methyl dibenzothiophene (4E6MDBT) in a fixed-bed reactor at $T = 598$ K, $P = 5.0$ MPa, and WHSV $= 46.4\ h^{-1}$. The catalysts were characterized by S_{BET}, XRD, DRS, FTIR spectroscopy of the framework vibration, DRIFTS in the OH region, ^{1}H-NMR, FT-IR spectroscopy of adsorbed NO and pyridine, XPS, and TGA. All Ti-containing catalysts showed higher activity than the Ti-free CoMo/HMS sample. The catalyst with a Si/Ti molar ratio of 40 is the most active. The HDS of 4E6MDBT over the Ti-free catalyst proceeds mainly via the dealkylation (DA) route, and then HDS of the more reactive DBT occurs. After Ti-incorporation into the HMS material, additional acid-catalyzed isomerization occurs, followed by direct HDS and HYD. Based on the catalyst activity–structure correlation, the increase in HDS activity over the Ti-containing catalysts with respect to the Ti-free sample was attributed to increased CoS_2 and MoS_2 surface exposure, as well as increased Lewis and Brønsted acidity.
© 2006 Elsevier Inc. All rights reserved.

Keywords: HMS and Ti(x)-HMS supports; CoMo catalyst; HDS of 4-ethyl-6-methyl dibenzothiophene; Physicochemical characterization

1. Introduction

Hydrodesulfurization (HDS) of petroleum fractions is one of the most important reactions in the petroleum industry for producing clean fuels [1–3]. The petroleum industry is currently facing the problem that a significant part of the reserves of some oil-producing countries consists of heavy oil fractions with high sulfur, nitrogen, (poly)-aromatic, and metal content. Often the content of dibenzothiophenes (DBT), and among them, 4-methyl dibenzothiophene (4-MDBT)-4,6-dimethyl dibenzothiophene (4,6-DMDBT), or 4-ethyl-6-methyl dibenzothiophene (4E6MDBT) is high. These compounds are very refractory toward desulfurization [4–7]. In particular, the desulfurization of methyl-substituted DBT compounds is a serious challenge in the production of low-sulfur fuels.

Co(Ni)–Mo-based sulfides supported on γ-Al_2O_3 are generally used as commercial catalysts for hydroprocessing [8]. However, these catalysts are not able to achieve deep HDS of alkyl-substituted DBT. The difficulty in converting alkyl-substituted DBT over CoMo/Al_2O_3 catalysts is due to the steric hindrance of the methyl groups, especially when both occupy the 4 and 6 positions, which hinders adequate interaction of the sulfur atom with the catalytically active site. In contrast with DBT, which is converted predominantly via the direct desulfurization (DDS) route, 4,6-DMDBT, 4,6-DEDBT, and 4E6MDBT react mainly via the hydrogenation (HYD) route, yielding tetrahydro- and hexahydro-intermediates, followed by desulfurization [9–13]. Thus, the challenge is to engineer new catalysts that can eliminate the sulfur of the alkyl-substituted DBT. This aim can be achieved by the hydrogenation of the aromatic rings or by dealkylation via C–C bond scission [10,14].

A number of studies have been reported on the deep HDS of 4,6-DMDBT over Co(Ni)Mo/Al_2O_3 catalysts [11–17]; however, the HDS of 4E6MDBT has been reported only by Robinson et al. [9,10]. The paucity of studies is likely due

* Corresponding author. Fax: +52 5556234165.
E-mail address: todor@servidor.unam.mx (T. Halachev).
[1] http://www.icp.csic.es/eac/index.htm.

0021-9517/$ – see front matter © 2006 Elsevier Inc. All rights reserved.
doi:10.1016/j.jcat.2006.06.008

to the fact that the 4E6MDBT reagent is not commercially available. Robinson et al. [9] reported a higher hydrogenation/hydrogenolysis ratio in the HDS of 4E6MDBT over CoMo catalysts supported on Al_2O_3, Al_2O_3–SiO_2, and activated carbon. Judging from their activity results, these authors concluded that CoMo catalysts likely are not suitable for a new generation of deep desulfurization catalysts. Later, the same authors [10] found that NiW supported on amorphous silica–alumina (ASA) was more active than NiMo/ASA or NiMo/Al_2O_3 in the HDS of 4E6MDBT due to the greater hydrogenation activity of W compared with Mo. The authors ascribed the higher activity on the acid support to the C–C bond scission either before or after the desulfurization step [10].

Landau et al. [14] and Isoda et al. [17] studied the effect of modifying the Al_2O_3 support by adding HY zeolite on the activity of CoMo catalysts in the HDS of 4,6-DMDBT. They found that steric hindrance was diminished by the migration of methyl groups in the aromatic ring, but the reactants were cracked simultaneously due to the acidic nature of the catalysts [14,17]. They observed 80% total conversion of 4,6-DMDBT over the CoMo/Al_2O_3 catalyst modified by HY zeolite. These results indicate that cracking reactions occur via two routes: scission of the C–C bond of the benzene rings (with selectivity toward these products of ca. 90%) and demethylation of the benzene rings. The HDS rate of DMDBT was about three times higher than that of the CoMo/Al_2O_3 catalyst. Kwak et al. [16] studied the effect of modifying alumina acidity by adding phosphorus to CoMo catalysts in the HDS of 4,6-DMDBT and found that at a P_2O_5 content of 0.5 wt%, catalytic activity increased due to the better dispersion of the molybdenum species. These authors proposed that an increase in Brønsted acidity allows migration of the methyl groups in 4,6-DMDBT, thus reducing steric hindrance during adsorption of the compound on the catalyst surface.

It is well known that the hydrogenation route suffers severe inhibition in the presence of aromatic hydrocarbons, such as naphthalene and tetraline, in gas-oil. Isoda et al. [15] studied the selectivity of the HDS of 4,6-DMDBT in the presence of naphthalene over CoMo-, Ru-, and ternary Ru–CoMo/Al_2O_3 blend catalysts and found that the sulfided ternary catalyst exhibited an excellent HDS activity of 4,6-DMDBT with no excess hydrogenation of naphthalene. This result was explained by the moderated steric hindrance and enhanced reactivity of the S atom when the Ru promoter was used. RuS_2 on Al_2O_3 was the site for the selective hydrogenation of 4,6-DMDBT, whereas the Co–Mo–S phase was the site for its desulfurization. Bataille et al. [12] studied the promoter effect of Co or Ni on the HDS activity of Mo/alumina catalysts in the HDS of DBT and of 4,6-DMDBT and observed significant enhancement of the DDS pathway in the HDS of DBT compared with that in the HDS of 4,6-DMDBT over the promoted catalyst. They therefore concluded that the main effect of the Co promoter on the HDS of DBT was to increase the rate of C–S bond cleavage. This effect was attributed to the promoter's enhancement of the basicity of certain sulfur anions shared between Mo and the Co promoter.

There is also an important body of work on the role played by the support in the dispersion and stacking of MoS_2 particles, as well as in the local structure and electronic properties of the CoMoS catalysts. Our earlier results [18] showed that incorporation of Ti into hexagonal mesoporous silica (HMS) enhanced the hydrogenation route of CoMo hydrotreating catalysts tested in the HDS of DBT. The higher catalytic activity of the Ti-modified catalysts compared with the Ti-free sample was attributed to better dispersion of the active species on the surface of the Ti-HMS support, higher concentration of octahedral Co^{2+} species, higher value of the sulfide Co/Mo ratio, and the specific degree of sulfidation of the Co particles, characterized by specific electronic properties, which promote both the DDS and HYD routes in the HDS of DBT. These results led us to study applications of CoMo/Ti-HMS catalysts in the less well-described reaction of HDS of 4E6MDBT.

In the present work, hexagonal mesoporous materials with wormhole framework structures (HMS), with Si/Ti molar ratios of 80, 40, and 20, were used as supports for CoMo catalysts. The CoMo formulation was chosen over the NiMo formulation because the former is less prone to sulfur poisoning [19]. The catalysts were tested in the reaction of HDS of 4E6MDBT in a fixed-bed flow reactor. The degree of catalytic deactivation was also evaluated. The catalysts were characterized by N_2 adsorption–desorption at 77 K (S_{BET}), X-ray diffraction (XRD), Fourier transform infrared (FTIR) spectroscopy of the framework vibrations, diffuse reflectance infrared Fourier transform spectroscopy (DRIFTS) in the OH region, H nuclear magnetic resonance (^{1}H-NMR), FTIR spectroscopy of adsorbed NO and pyridine, X-ray photoelectron spectroscopy (XPS), and thermogravimetric analysis (TGA).

2. Experimental

2.1. Synthesis of the HMS and Ti-HMS supports

Hexagonal mesoporous silica (HMS) was synthesized by the neutral S^0I^0 templating route, proposed by Tanev and Pinnavaia [20,21], which is based on hydrogen bonding and self-assembly between neutral primary amine surfactants (S^0) and a neutral inorganic precursor (I^0). The Ti-HMS material was prepared following a procedure similar to that described by Gotier and Tuel [22] using dodecylamine ($C_{12}H_{25}NH_2$, Aldrich 98%) as surfactant, but with the reaction mixture slightly modified by addition of the swelling agent mesitylene (C_9H_{12}, Aldrich 98%), as first proposed by Kresge et al. [23]. The Ti(x)-HMS material was synthesized with Si/Ti atomic ratios (x) of 20, 40, and 80. The reaction products were filtered, washed with distilled water, and dried at room temperature for 24 h, then dried at 378 K for 2 h. Subsequently, the samples were calcined at 823 K for 3.5 h in air, with a heating rate of 2.5 K min^{-1}.

2.2. Catalyst preparation

The catalysts were prepared by successive impregnation using the pore-filling method. First, molybdenum was introduced from an aqueous solution of ammonium heptamolybdate [$(NH_4)_6Mo_7O_{24}$, Aldrich 99%]. The obtained samples were dried at room temperature for 18 h and then at 378 K

Table 1
Chemical composition and textural properties of the pure supports, calcined and sulfided catalysts

Sample	S_{BET} ($m^2\,g^{-1}$)		Pore diameter (nm)		Average pore volume ($cm^3\,g^{-1}$)		Mo (wt%)	Co (wt%)	TiO_2[a] (wt%)
Supports									
HMS	990		3.1		1.32		–	–	0.0
Ti(80)-HMS	975		3.3		1.32		–	–	1.61
Ti(40)-HMS	961		3.4		1.74		–	–	3.18
Ti(20)-HMS	952		3.6		1.37		–	–	6.16
Catalysts	Cal.	Sul.	Cal.	Sul.	Cal.	Sul.			
CoMo/HMS	432	318	2.7	2.5	0.74	0.71	9.0	3.0	0.0
CoMo/Ti(80)-HMS	554	492	3.4	3.4	0.52	0.80	9.0	3.0	1.37
CoMo/Ti(40)-HMS	665	558	3.4	3.4	0.99	0.99	9.0	3.0	2.67
CoMo/Ti(20)-HMS	534	484	3.5	3.4	0.58	0.84	9.0	3.0	5.27

[a] TiO_2 wt% was derived from atomic absorption analysis.

for 2 h. Then the samples were calcined at 773 K for 4.5 h, with this temperature reached within 3.5 h, after which the solution with the corresponding concentration of cobalt nitrate [$Co(NO_3)_2$), Aldrich 98%] was added. Subsequently, the samples were dried at room temperature for 18 h and then at 378 K for 2 h, followed by calcination at a 773 K for 4.5 h, with this temperature reached within 3.5 h. Table 1 gives the chemical composition and denomination of the catalysts.

2.3. Characterization methods

2.3.1. N_2 adsorption–desorption isotherms at 77 K

The textural properties of the supports and the sulfided catalysts were determined by N_2 adsorption–desorption isotherms at 77 K on a Micromeritics ASAP 2000 device. The catalysts were sulfided ex situ in a U-shaped glass reactor under the same conditions as described in the section on catalytic activity tests. After sulfidation, the sample was cooled to room temperature under N_2 flow, then transferred into the Micromeritics apparatus in an argon atmosphere without being exposed to air. Before the experiments, the supports and sulfided catalysts were degassed at 543 K in vacuum for 5 h. The volume of the adsorbed N_2 was normalized to the standard temperature and pressure. Specific surface area (S_{BET}) was calculated by the BET equation applied to the range of relative pressures $0.05 < P/P^0 < 0.30$. The average pore diameter was calculated by applying the Barret–Joyner–Halenda (BJH) method to the adsorption branches of the N_2 isotherms. The cumulative pore volume was obtained from the isotherms at $P/P^0 = 0.99$.

2.3.2. FTIR study of framework vibrations

Framework IR vibrations in the range of 400–1400 cm^{-1} were collected on a Nicolet 510 FTIR spectrophotometer working with a resolution of 4 cm^{-1}. Wafers of the samples were prepared by diluting 2 mg of the corresponding sample in 140 mg of KBr at pressure of 7×10^3 $kg\,cm^{-2}$. The spectra were collected after 100 scans using a KBr spectrum as a background.

2.3.3. DRIFT spectra in the OH region

The DRIFTS spectra of the calcined catalysts were recorded on a Bruker IFS spectrophotometer, using a Harrick HVC-DRP cell that allows in situ treatment of the samples. A 30-mg portion of the finely ground sample was placed in the sample holder and heated at 623 K for 30 min in a flow of helium, with this temperature reached within 2.5 h. The DRIFT spectra were recorded at room temperature with a resolution of 4 cm^{-1} after 500 scans using a KBr spectrum as a background.

2.3.4. ^1H-NMR

Solid-state CP MAS ^{1}H-NMR measurements were recorded on a Brucker AV 400 WB spectrometer. The dried, powdered samples were loaded into a BL_4 X/Y/^{1}H 4-mm multinuclear probe and spun at 5 kHz according to the following protocol: $\pi/2$ pulse, 7 μs; CP contact time 2 ms; 1700 scans. An internal reference of the spectrometer was used to calculate chemical shifts. Before the experiments, the samples were dried at 520 K for 2 h.

2.3.5. FTIR spectroscopy of adsorbed NO and pyridine

Self-supporting wafers of the oxide catalysts with a thickness of 12 $mg\,cm^{-2}$ were prepared by pressing (7×10^3 $kg\,cm^{-2}$) the powdered sample during 10 min. The wafers were introduced into a special IR cell with greaseless stopcocks and KBr windows, after which the samples was sulfided in situ with a 10% H_2S/H_2 mixture at 673 K at a rate of 60 $ml\,min^{-1}$, with this temperature reached in 3 h. Then the samples were degassed under 10^{-5} mbar at 723 K for 1 h. Once the samples were cooled to ambient temperature, they were exposed to 20 mbar of NO for 5 min, after which the spectrum was recorded on a Nicolet 510 FTIR spectrophotometer at a resolution of 4 cm^{-1}. Then the samples were degassed under 10^{-5} mbar at 673 K for 2 h to achieve total desorption of the NO molecules, and the spectrum of the catalyst was recorded. The IR spectrum of the adsorbed NO was obtained by subtracting the spectrum of the corresponding catalyst, degassed under vacuum at 673 K. Adsorption of pyridine was performed on sulfided samples using the same IR cell. The samples were degassed at 723 K for 2 h and cooled to 393 K before contact with ca. 2 Torr of pyridine. Then IR spectra were recorded after physically adsorbed pyridine (10^{-5} Torr) was evacuated at 393 K for 0.5 h.

2.3.6. XPS studies

The XPS spectra of the calcined, freshly sulfided (673 K), and used catalysts were recorded on a VG Escalab 200R spectrometer equipped with a hemispherical electron analyzer and a Mg$K\alpha$ ($h\nu = 1253.6$ eV) X-ray source. The oxide samples were first placed in a copper holder mounted on a sample rod in the pretreatment chamber of the spectrometer, and then degassed at 403 K for 1 h before being transferred to the analysis chamber. The freshly sulfided and used CoMo catalysts were kept under *i*-octane to avoid exposure to air, and then introduced into the preparation chamber. All supports and catalysts were degassed at 10^{-5} mbar and then transferred to the ion-pumped analysis chamber, where the residual pressure was $<7 \times 10^{-9}$ mbar during data acquisition. The binding energies (BEs) were referenced to the C 1s peak (284.9 eV) to account for the charging effects. The accuracy of the BE values is ±0.1 eV. The areas of the peaks were computed after the experimental spectra were fitted to Gaussian/Lorentzian curves and the background was removed (Shirley function). Surface atomic ratios were calculated from the peak area ratios normalized by the corresponding atomic sensitivity factors.

2.3.7. Catalytic activity measurements

The gas-phase HDS of 4E6MDBT was performed in a high-pressure laboratory-scale setup equipped with a stainless steel fixed-bed catalytic reactor. The 4E6MDBT was diluted in decaline to obtain a 0.2 wt% solution, and the mixture was injected (0.25 ml min^{-1}) by a high-pressure pump (HPLC Knauer) into a hydrogen stream (60 ml min^{-1}). The reaction was carried out at 598 K and 5 MPa of total pressure under a H_2 flow rate of 7 l (STP) h^{-1} and a WHSV of 46.4 h^{-1}. Then 0.25 g of the catalyst, diluted with 5 g of SiC, was introduced into the reactor. Before being activated, the catalyst was dried under a N_2 flow of 100 ml min^{-1} at 423 K for 0.5 h. Then the catalyst was sulfided in situ at atmospheric pressure by a mixture of 10 vol% of a H_2S:H_2 at a rate of 60 ml min^{-1} for 4 h at 673 K (isothermal). After sulfidation, the catalyst was purged under a N_2 flow of 100 ml min^{-1} at 473 K for 0.5 h, then stored overnight under a N_2 flow of 3 ml min^{-1}. Before the experimental runs, the N_2 pressure was increased to the desired value, and the catalytic bed was heated to the reaction temperature. Owing to the high boiling point of the reactant and the solvent, on-line analysis of the reaction products was not convenient; consequently, the reactor effluents were condensed, and liquid samples were periodically collected and analyzed by gas-liquid chromatography (Varian chromatograph Model Star 3400 CX) using a flame ionization detector (FID) and a 30 m × 0.53 mm DB-1 column (100% methyl-polysiloxane, J&W Scientific) as a stationary phase. A commercial hydrodesulfurization CoMo/Al_2O_3 catalyst (AKZO KF-752; 3.8 wt% Co; 14.2 wt% Mo) was used as a comparison.

2.3.8. Thermogravimetric analysis (TGA)

The amount of coke deposited on the used catalysts was determined using a TGA/SDTA851^e device (Mettler Toledo) to measure the weight change in the coked catalysts during oxidation. The burning of coke was carried out by raising the sample temperature to a final temperature of 1073 K at a rate of 10 K min^{-1} in a 20% O_2/N_2 mixture.

3. Results

3.1. Nitrogen adsorption–desorption

The structure parameters, including specific area (S_{BET}), cumulative pore volume (V_p), pore diameter of the pure supports, and CoMo catalysts after calcination and sulfidation, are listed in Table 1. The Ti-free HMS material has the highest specific area. The specific area of the HMS support decreases with the incorporation of titanium, whereas the pore diameter increases with increasing Ti content. The specific area values follow the order HMS > Ti(80)-HMS > Ti(40)-HMS > Ti(20)-HMS, whereas the pore diameter follows the order HMS < Ti(80)-HMS < Ti(40)-HMS < Ti(20)-HMS. In contrast to the average pore diameter values, the effect of Ti concentration on the average pore volume is not linear. The highest average pore volume is observed on the sample with a Si/Ti atomic ratio of 40.

The deposition of Co and Mo species caused an additional decrease of the specific area. The highest decrease in the surface area is observed in the Ti-free sample. The values of S_{BET} follow the order CoMo/Ti(40)-HMS > CoMo/Ti(80)-HMS > CoMo/Ti(20)-HMS > CoMo/HMS. The highest decrease in the specific area of the CoMo/HMS catalyst might indicate that, under the conditions of impregnation and calcination used in this work, larger CoMo particles are formed, blocking the pores. The pore diameter decrease is more pronounced in the Ti-free HMS sample, whereas it is practically the same in the Ti-containing samples as in the pure supports. This last result looks rather strange at first glance. A possible explanation for it is that the supported species are located predominantly on the external surface of the Ti-containing supports. This suggestion is supported by the significant decrease in the average pore volume values due to blocking of the pores between the particles of the supports.

The values of the structural parameters of the sulfided samples indicate that after sulfidation, the S_{BET} areas decrease in comparison to those of the oxide catalysts. The following trend is observed: CoMo/Ti(40)-HMS > CoMo/Ti(80)-HMS ≈ CoMo/Ti(20)-HMS > CoMo/HMS. It is noteworthy that the pore diameter of the sulfided Ti-containing samples does not change after sulfidation, supporting the suggestion that in these samples the active species are not located inside the pores of the wormhole structure of the supports. Moreover, sulfidation does not lead to changes in the average pore volume values of the Ti-free and the Si/Ti = 40 samples, whereas the Si/Ti = 20 and Si/Ti = 80 samples show significantly increased values. The origin of this behavior is not very clear, but it demonstrates that the latter samples undergo strong changes in their structural parameters during sulfidation, which should be reflected in their catalytic performance.

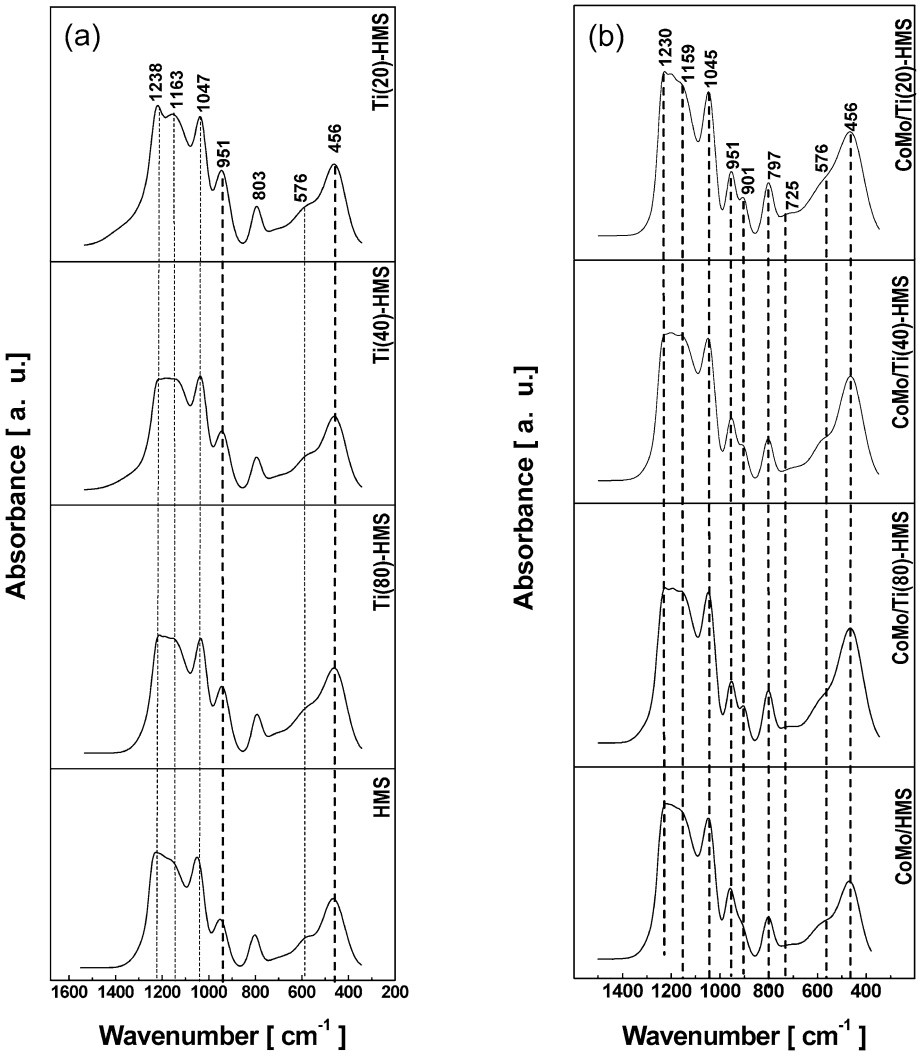

Fig. 1. FT-IR spectra of the framework vibration of the pure supports (a) and the calcined CoMo/Ti(x)-HMS catalysts (b).

3.2. FT-IR and DRIFTS spectra of the samples

Figs. 1a and 1b show the IR spectra of the pure supports and of the calcined catalysts in the range of 400–1400 cm^{-1}. The bands at 456, 576, 803, 951, 1047, 1163, and 1238 cm^{-1} are observed in all supports irrespective of the presence of titanium (Fig. 1a). The bands at 456, 576, 803, and 1163 cm^{-1} are assigned to Si–O–Si vibrations [24] and are generally observed in this type of material. The band at 951 cm^{-1} is assigned to silanol groups [25,26], the band at 1047 cm^{-1} is assigned to external linkage [24], and the intensive band at 1238 cm^{-1} is assigned to adsorbed CO_2. Note that no Ti–O–Si or Ti–O–Ti vibrations are observed. A difference in the intensity of the band of the silanol groups is seen with increasing Ti content, in the order Ti-(20)HMS > Ti(40)-HMS > Ti(80)-HMS > HMS. Note that the prevailing silanol groups in these materials are the single ones, not connected with H bonding between them. It seems that with the increase in Ti content comes an increase in the number of single silanol groups, due to the presence of more surface Ti ions, which break the H bonding between the silanol groups.

The spectra of the calcined catalysts (Fig. 1b) are similar to those of the pure supports, and no significant changes in the band positions are observed. Generally, the intensity of all bands decreases with deposition of the catalytically active species. The most significant decreases are observed for the band of the single silanol groups and for the external linkage band. This should be expected keeping in mind that the deposition of the active components is related to the disappearance of silanol groups. However, we cannot distinguish from these spectra whether or not Ti–OH groups are also involved in the interaction with the supported active species. The presence of a new band at 901 cm^{-1} is observed in all catalysts; this band is generally assigned to Mo–O–Mo vibrations [27]. The intensity of this band follows the order Ti(20)-HMS > Ti(80)-HMS > Ti(40)-HMS > HMS. Clearly, the titanium effect is not linear.

Fig. 2 shows the DRIFT spectra of the supports and the catalysts in the 3000–4000 cm^{-1} interval, recorded after heating of the samples at 623 K for 30 min in a He flow. All spectra of the supports are characterized by an intensive band at ca. 3743 cm^{-1}, which has been assigned to isolated silanol groups

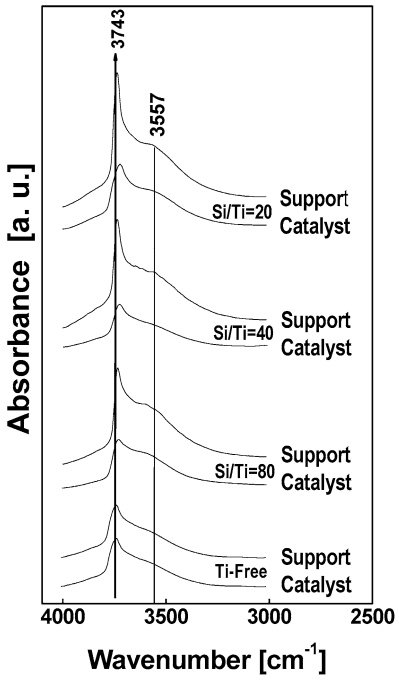

Fig. 2. DRIFT spectra in the OH region of the pure supports and calcined catalysts.

[26]. Note that the intensity of this band strongly increases with increasing Ti content in the supports. Moreover, the width of the band decreases with Ti content. This result is in agreement with the FTIR spectra and has the same interpretation. This band is rather asymmetric in the direction of lower wave numbers. This effect is due to the superimposition of the band of the H-bonded bands of the silanol groups, normally observed at approximately 3650 cm^{-1} [28] and the band of the Ti–OH groups, which appears at approximately 3690 cm^{-1}. The narrowing of the peak of the isolated silanol groups with the increase of the Ti content in the supports is due to the decrease in the number of H-bonded silanol groups and their smaller contribution to the superimposition of the bands in the broad tail of this band. At first sight it might appear that the number of the Ti–OH groups in the pure supports also decreases raising the Ti content. However, a careful examination of the intensity of the shoulder at approximately 3690 cm^{-1} indicates that the following order of intensities is valid: Ti(20)-HMS > Ti(40)-HMS > Ti(80)-HMS. We should also note that the band of the isolated silanol groups of all Ti containing supports, as should be expected, is shifted by 12 cm^{-1} to lower wave numbers, indicating a homogeneous distribution of the Ti^{4+} ions exposed on the surface in the siliceous matrix.

The deposition of the catalytically active components on the supports leads to a strong decrease of the intensity of the band of the isolated silanol groups. For the calcined catalysts, the intensity of this band follows the order: CoMo/Ti(40)-HMS > CoMo/Ti(20)-HMS > CoMo/Ti(80)-HMS > HMS. This order, although it does not include the interaction with the Ti–OH groups might be indicative of the dispersion of the active species, as far as the silanol groups are involved in the interaction with the precursors. We should note that the effect of the Ti content on the decrease of the band intensity of isolated silanol groups is not linear, indicating that the sample with Si/Ti = 40 atomic ratio has some special characteristics, which should be reflected in its catalytic behavior.

Besides, this band is also shifted to lower wave numbers in comparison to its position in the Ti-free sample (3724, 3712 and 3706 cm^{-1} for the CoMo/Ti(80)-HMS, CoMo/Ti(40)-HMS, CoMo/Ti(20)-HMS samples, respectively). In this aspect the effect of the Ti content is linear, contrary to the effect on the decrease of the intensity of this band. This discrepancy might has its explication in the complex relation between the interaction of the active species with the silanol groups on one hand and the interaction with the Ti–OH groups on the other hand vs the Ti content in the samples. To clarify this point we carried out a ^{1}H-NMR study of the pure supports and the catalysts.

3.3. ^{1}H-NMR spectra

The ^{1}H-NMR spectra of the supports and the CoMo catalysts were recorded in order to obtain quantitative information about the interaction between the metals ions and the hydroxyl groups on the support without the difficulties associated with the DRIFT spectroscopy. The ^{1}H-NMR spectra of the supports and calcined catalysts are shown in Figs. 3a and 3b, respectively. The HMS support, where the only component is SiO_2, presents an asymmetrical band centered at 1.20 ppm assigned to isolated –Si–OH groups [29]. The asymmetric form in the Ti-free support can be explained with the presence of the H-bonded silanol groups. In the presence of Ti the intensity of the signal is higher than that of the pure HMS support and follows the order Ti(20)-HMS > Ti(40)-HMS > Ti(80)-HMS > HMS. This order, as should be expected, coincides with the order of intensities observed in the DRIFT spectra of the isolated silanol groups. The introduction of the Ti ions into the supports decreases the asymmetric shape of the signal of the isolated silanol groups. Besides, a new band at 2.91 ppm appears in the Ti containing supports. The intensity of this signal increased with the increase of the Ti content and reflects the increasing amount of Ti–OH groups.

The intensity of the signal of the isolated silanol groups at 1.20 ppm in the CoMo/HMS catalysts strongly decreases in comparison to that of the pure HMS support. However, it preserves its asymmetric form indicating that the interaction of the active species with the support is carried out predominantly with the isolated silanol groups. The intensity of this signal also decreases in the Ti-containing catalysts. The intensity of the signal of the isolated silanol groups follows the order CoMo/Ti(40)-HMS < CoMo/Ti(80)-HMS < CoMo/Ti(20)-HMS < CoMo/HMS. One should note that the signal of the Ti–OH groups almost disappears in the samples with Si/Ti = 80 and 40 molar ratio. Surprisingly, this signal is preserved in the sample with the highest Ti content, although its intensity decreases in comparison to that of the Ti(20)-HMS support. Obviously, the effect of the Ti content is not linear and significant changes in the reactivity of both the silanol and Ti–OH groups are observed. This can be attributed to the specific electronic properties in the different supports. One could ex-

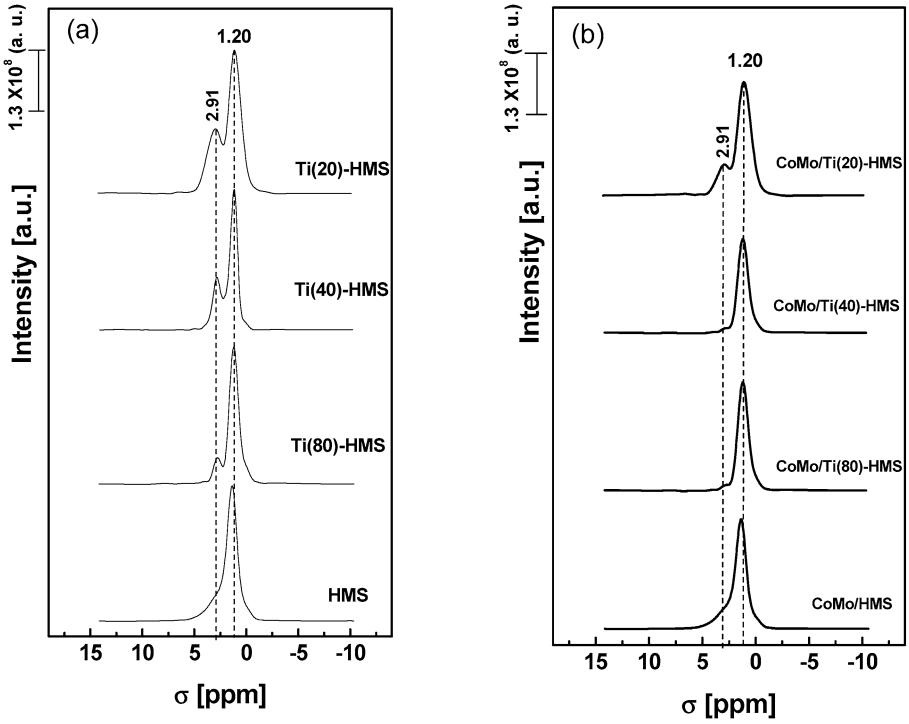

Fig. 3. ^{1}H NMR spectra of the pure supports (a) and calcined CoMo/Ti(x)-HMS catalysts (b).

pect that these differences would be reflected in the catalytic properties of the samples.

3.4. FTIR of adsorbed NO on the sulfided catalysts

The infrared spectroscopy of chemisorbed NO was used to identify the chemical state and the nature and surface exposure of cobalt and molybdenum ions after catalyst sulfidation at 673 K. Fig. 4 shows the FTIR spectra of adsorbed NO on the freshly sulfided catalysts. The deconvolution of the IR bands associated with N=O adsorbed on Co sites indicates that not all cobalt species are completely sulfided. Thus, the doublet bands around 1862 and 1791 cm^{-1} could be assigned respectively as due to the symmetric and anti-symmetric stretching vibrations mode of NO adsorbed on the CoS_2 species [30–34], whereas the absorption bands around 1873 and 1802 cm^{-1} are assigned respectively to the symmetric and anti-symmetric stretching frequencies of dinitrosyl species adsorbed on the Co^{2+} ions surrounded by oxygen ($Co(NO)_2$). Noticeably, the bands of both doublets are rather broad, which indicates that cobalt particles of different size and form with different number of atoms in the edges, planes and in the vertices participate in the adsorption of the NO.

To obtain information regarding the surface exposure of sulfided Co species adsorbing NO, which are often related to the amount of sulfur vacancies associated to the active sites, the integrated absorbance of the bands at ca. 1862 and 1791 cm^{-1} was compared. It is obvious from Fig. 4 that all Ti-containing catalysts show larger surface exposure of sulfided Co species than the Ti-free sample. The following order of the values of the surface areas (numbers in brackets) below the two peaks of NO adsorbed on sulfided Co species is observed: CoMo/HMS (4.6) < CoMo/Ti(20)-HMS (5.77) < CoMo/Ti(80)-HMS (5.91) < CoMo/Ti(40)-HMS(6.42). The same order is valid for the amount of oxidized Co species: CoMo/HMS (0.941) < CoMo/Ti(20)-HMS (1.38) < CoMo/Ti(80)-HMS (1.67) < CoMo/Ti(40)-HMS (2.20). Obviously the CoMo/Ti(40)-HMS sample has the highest amount of surface exposed sulfided and oxidized Co species. This is possible if this sample has much higher dispersion than the other samples.

The bands at approx. 1750 and 1618 cm^{-1} are assigned to stretching vibrations of N=O adsorbed on MoS_2 [31,33–35]. One can note that the intensities of these bands are much lower than those of the NO adsorbed on the cobalt species. Taking in account that the concentration of Mo is much higher than that of Co and that its dispersion is relatively high and no MoO_3 particles are detected by XRD (data no shown here), one might conclude that the adsorption of NO takes place predominantly on the Co species or that some of the Mo ions are covered by Co species. The broad bands are also indicative of the presence of Mo particles of different size and shape.

A small shift to higher wave numbers of the asymmetric band is observed in the sulfided CoMo/Ti(80)-HMS and CoMo/Ti(40)-HMS samples. This shift indicates that in these two samples the back donation of electrons from Mo to the antibonding orbital of NO is higher than that in the CoMo/Ti(20)-HMS and CoMo/HMS samples. One could expect that significant differences in the catalytic activities of the two groups of samples should exist. Besides, the intensity of this band for the CoMo/Ti(40)-HMS sample is the highest among all samples, which indicates that more Mo ions are exposed on the surface of this sample. Indeed, the intensities (areas) of

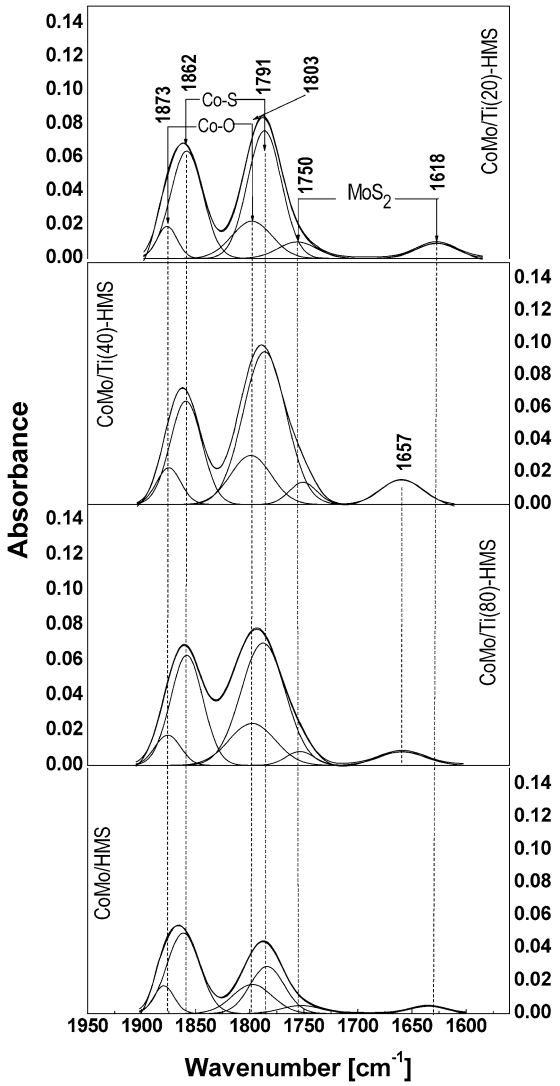

Fig. 4. IR spectra of NO adsorbed on the sulfided CoMo/Ti(x)-HMS catalysts.

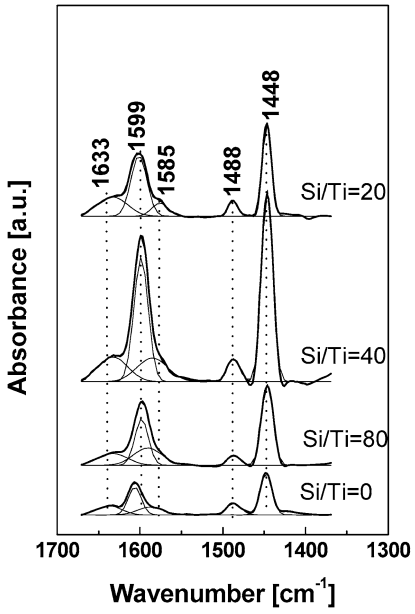

Fig. 5. IR spectra of adsorbed pyridine on the sulfided CoMo/Ti(x)-HMS catalysts.

Table 2
Area of the bands at 1633 cm^{-1} (B) and 1448 cm^{-1} (L) of pyridine adsorbed on the sulfided CoMo/Ti(x)-HMS catalysts

Acid site	Sample			
	CoMo/ HMS	CoMo/ Ti(80)-HMS	CoMo/ Ti(40)-HMS	CoMo/ Ti(20)-HMS
Brønsted site (1633 cm^{-1})	0.85	1.35	2.78	2.18
Lewis site (1448 cm^{-1})	2.69	5.60	11.14	4.11

the bands follow the order CoMo/Ti(40)-HMS < CoMo/Ti(20)-HMS < CoMo/Ti(80)-HMS < CoMo/HMS.

3.5. FTIR of adsorbed pyridine on the sulfided catalysts

The FTIR spectra of pyridine adsorbed on the sulfided catalysts are presented in Fig. 5. The identification of the bands is made following the assignment published by Wang et al. [36,37] and Ward [38]. The intensive bands at 1448 and 1599 cm^{-1} belong to the anti-symmetric and symmetric vibrations of pyridine adsorbed on Lewis (L) acid sites, respectively. The weak band at 1488 cm^{-1} is assigned to contributions from symmetrical vibrations of both L and Brønsted (B) acid sites. The shoulder at approximately 1585 cm^{-1} is assigned to the anti-symmetric vibrations in the plane of pyridine on L sites.

We should note than the band at 1538 cm^{-1} assigned to the anti-symmetric vibration of pyridine on B acid sites is not observed. However, the broad shoulder at approximately 1633 cm^{-1} normally assigned to the symmetric vibration of pyridine on B sites, is clearly visible. The absence of the anti-symmetric vibration and the relatively weak symmetric vibration on the B sites is most probably due to the degassing of the samples before collecting the spectra. This treatment leads to removal of the –SH and –OH groups and the signal from the B acid sites strongly decreases. The values of the surface area below the bands at 1633 cm^{-1} (B) and 1448 cm^{-1} (L) are given in Table 2. It is obvious that the incorporation of Ti-ions into the HMS framework strongly increases both the B and L acidity of the samples in comparison to the Ti-free catalyst. The highest acidity (both B and L) is observed on the sample with Si/Ti ratio of 40. The sulfur vacancies associated with the Co and Mo ions are expected to have L acid character. The strong increase of the L acidity of the S/Ti = 40 sample indicates that the number of sulfur vacancies in this sample is higher in comparison to the other samples. This result is in an agreement with the NO adsorption FTIR results, which showed that the intensities of the bands associated with NO adsorption on Co and Mo sulfided species are higher in this sample. One can note that the orders of the amounts of exposed sulfided and oxidized Co species, as determined by NO adsorption, coincide with the order of the amount of L acid sites.

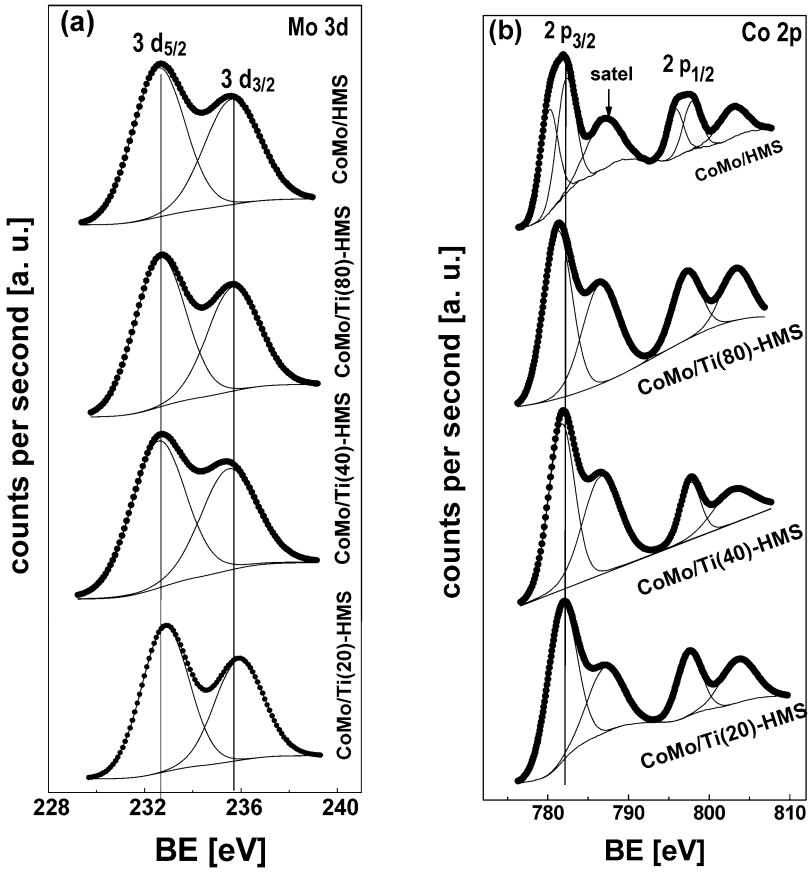

Fig. 6. XPS spectra of the calcined CoMo/Ti(x)-HMS catalysts: (a) Mo 3d, (b) Co 2p.

3.6. XPS spectra of the calcined, sulfided and used catalysts

3.6.1. Calcined and freshly sulfided catalysts

Figs. 6 and 7 show the Mo 3d (a) and Co 2p (b) core level spectra of the calcined and used catalysts, respectively. The spectra of the freshly sulfided catalysts were published in [18]. The binding energies (BE) of the samples are presented in the Table 3. For comparison, Table 3 also contains the BE of the freshly sulfided samples. The values of the BE of the Mo $3d_{5/2}$ in all calcined sample is very close to that of MoO_3 [39]. One can note that in the presence of Ti the BE values decrease, in comparison to the Ti-free sample. The lowest BE is observed for the sample with Si/Ti atomic ratio of 40. This result implies that in this catalyst some excess of electrons exists in the Mo ions in comparison to the others Ti-containing catalysts. The changing values of the BE of the Mo^{6+} ions might also reflect the presence of molybdenum particles of different size and form, as indicated by our DRS results in the UV range [18]. The surface atomic ratios of the calcined and used catalysts are given in Table 4. The atomic ratios of the freshly sulfided catalysts were published in [18]. In order to follow the evaluation of the samples from the oxide state to the freshly sulfided and finally to the state after work, we have additionally included in Table 4 the results on the freshly sulfided samples. One can note that the amount of exposed Mo^{6+} ions in the calcined catalyst increases gradually with the increase of the Ti content. Obviously, the presence of Ti increases the dispersion of the supported species. We should note that this effect of the Ti-ions on the increase of the surface exposure of the Co ions is stronger than that on the Mo species. The CoMo/Ti(40)-HMS sample shows the highest Co/Si value. The Co/Mo values follow the same trend and again the highest value is observed for the CoMo/Ti(40)-HMS sample. It is also interesting to note that the amount of Ti ions exposed on the surface increases, as expected, with the increase of the Ti content, but in the calcined catalysts the Ti/Si ratio is much higher than that in the pure supports. This enrichment of the surface with Ti ions takes place during the complex physicochemical processes occurring during the impregnation and calcination of the supports.

The BE of the cobalt species in the oxide Ti-free catalyst reflects the presence of tetrahedral (782.7 eV) and octahedral (780.40 eV) cobalt species [39–41]. The signal of the tetrahedral Co species disappears in the Ti-containing samples. The increase of the Ti-content leads to an increase of the BE of the Co species. The highest value of the BE is observed for the sample with the highest Ti concentration. This result can be explained by the presence of some Co^{3+} ions in this sample [18]. The observed general increases in the BE values of the cobalt ions could be caused by electron transfer from Co to Ti or to Mo. If the transfer is from Co to Ti the values of the BE of the Ti^{4+} ions should change significantly. However, the Ti^{4+} BE values practically do not change, while the BE values of the Mo ions decrease. It seems that the electron transfer occurs

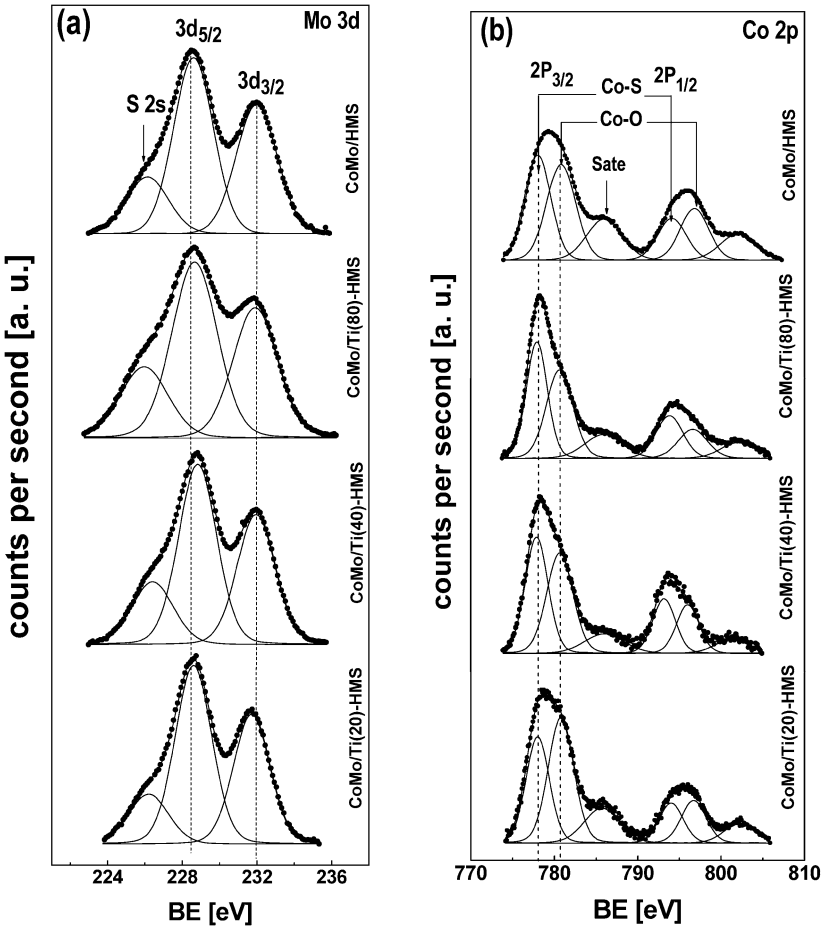

Fig. 7. XPS spectra of the used CoMo/Ti(x)-HMS catalysts: (a) Mo 3d and S 2s, (b) Co 2p.

Table 3
Binding energies (eV) of the calcined, freshly sulfided and used CoMo/Ti(x)-HMS catalysts

Sample	Mo $3d_{5/2}$		Co $2p_{3/2}$		Ti $2p_{3/2}$	S 2p
			Co(S)	Co(O)		
CoMo/HMS	Calc.	232.9	–	780.4 782.7	–	–
	Sulf.	227.6	778.2	780.9	–	161.2
	Used	228.7	778.0	780.8	–	161.7
CoMo/Ti(80)-HMS	Calc.	232.7	–	781.1	459.9	–
	Sulf.	228.0	778.1	780.8	459.9	161.1
	Used	228.6	778.0	780.8	459.8	161.5
CoMo/Ti(40)-HMS	Calc.	232.4	–	781.5	460.0	–
	Sulf.	228.2	778.1	780.6	460.0	161.3
	Used	228.4	778.0	780.8	460.0	161.6
CoMo/Ti(20)-HMS	Calc.	232.6	–	781.8	459.8	–
	Sulf.	227.6	778.1	780.4	459.8	161.2
	Used	228.6	778.0	780.8	459.9	161.7

from the Co ions towards the Mo ions. It is not clear from our results if this transfer takes please via an intimate contact between the Co and Mo ions or it proceeds via redistribution of the electron density through the support.

The BE of sulfur observed in the freshly sulfided catalyst is typical of S^{2-} ions and no sulfate species are observed. The BE of Mo in the freshly sulfided Ti-free catalyst is somewhat lower than the observed at 228 eV value of pure MoS_2 [42]. The BE of Mo gradually increases in the low and medium Ti-content samples and in the high Ti-content sample it drops down to the value of the Ti-free sample. The observed changes in the BE of Mo in the freshly sulfided samples is probably caused by different factors. The Mo species are partially adsorbed on the Ti ions in the samples with low and medium Ti content, whereas in the sample with high Ti content, the Mo species practically do not interact with the Ti–OH groups. The effect of some redispersion of the supported species during the sulfidation procedure, or a change in the morphology or orientation of the MoS_2 clusters, cannot be excluded [43]. Indeed, note that in the freshly sulfided catalysts, redispersion of the Mo species occurs, and the Mo/Si values are generally higher than in the oxide catalysts (Table 4). Changes in the number of corner, edge, and basal plane Mo atoms with different electronic densities in the different samples, where each type of Mo ion makes its own contribution to the total band position, form, and intensity, is most likely responsible for the observed changes in the BE values. The Co/Si values increase in the freshly sulfided Ti-free and Si/Ti = 20 samples but decrease in the other Ti-containing samples in comparison with the values of the oxide catalysts. It seems that the CoMo/Ti(20)-HMS catalyst manifests the high-

Table 4
Surface atomic ratios of the calcined, sulfided and used CoMo/Ti(x)-HMS catalysts

Sample	State of the sample	Mo/Si	Co/Si	Co/Mo	CoO/(CoO + CoS)	Ti/Si[a]	S/(Mo + Co)
CoMo/HMS	Calc.	0.011	0.0062	0.56	–	0.0 (0.0)	–
	Sulf.	0.013	0.0071	0.546	0.47	0.0	1.23
	Used	0.018	0.0103	0.572	0.46	0.0	1.25
CoMo/Ti(80)-HMS	Calc.	0.017	0.0144	0.850	–	0.012 (0.005)	–
	Sulf.	0.017	0.0109	0.641	0.53	0.008	1.41
	Used	0.023	0.0122	0.530	0.51	0.0105	1.51
CoMo/Ti(40)-HMS	Calc.	0.018	0.0209	1.160	–	0.022 (0.008)	–
	Sulf.	0.019	0.0203	1.068	0.58	0.011	1.34
	Used	0.026	0.0133	0.512	0.57	0.0161	1.43
CoMo/Ti(20)-HMS	Calc.	0.019	0.0202	1.060	–	0.031 (0.013)	–
	Sulf.	0.022	0.0207	0.941	0.51	0.019	1.16
	Used	0.021	0.0117	0.557	0.55	0.0323	1.29

[a] The Ti/Si atomic ratio of the support is given in parentheses.

est dispersion for both the Mo and the Co species; however, as we discuss later, this is not the most active catalyst.

As a result of these redispersion/sintering effects, the Ti/Si values decrease in all freshly sulfided catalysts compared with the oxide catalysts. It is also interesting to note that the Co/Mo values also decrease in all freshly sulfided samples in comparison with the oxide catalysts. The highest value is observed for the CoMo/Ti(40)-HMS sample in both oxide and freshly sulfided states.

The presence of Ti in the samples strongly influences the extent of sulfidation of the Co species in the freshly sulfided catalyst. The BE values of Co in the freshly sulfided catalyst indicate the presence of CoS_2 (778.1 ± 0.1 eV) [39] and oxide species (780.6 ± 0.1 eV) [18,43]. The increased Ti content shown in Table 4 results in a general increase in the amount of oxidized Co species in comparison with the Ti-free sample. The effect of Ti content is not linear, however, with the greatest amount of Co oxide species found in the Si/Ti = 40 sample.

3.6.2. *Used catalysts*

The BE values of Mo in the used catalysts generally increase compared with those in the freshly sulfided samples. It is interesting to note that this increase is the smallest for the CoMo/Ti(40)-HMS sample. This electron deficiency in Mo can be explained by the presence of excess sulfur. Indeed, the degree of sulfidation of all samples after time on stream is higher than that in the freshly sulfided catalysts, as shown in Table 4. Moreover, the BE values of S are higher in the used catalysts than in the freshly sulfided catalyst. The BE of the Co species are practically the same in the used catalysts and the freshly sulfided catalysts. We can conclude that the excess sulfur is predominantly bound to the Mo species and comes from the HDS process.

Some important changes occur in the samples during the reactions, as shown by the results in Table 4. The values of the Mo/Si ratio increase in all samples except the high-Ti concentration sample in comparison with the freshly sulfided catalysts. The highest value is observed in the sample with Si/Ti = 40. This result implies that redispersion of the Mo species occurs during the reaction. The behavior of the Co species is more complex. The Ti-free and the low-Ti content samples show the existence of some redispersion, whereas the other Ti-containing samples have Co/Si values much lower than those of the freshly sulfided catalysts. It seems that some sintering of the Co species occurs in these samples. Obviously, the effect of Ti is not linear, and these changes in the structure and electronic properties of the supported species should be manifested in the activity and selectivity of the samples.

The Ti/Si ratio increases in all samples as a result of the redispersion/sintering effects during the reaction. The Ti/Si value for the CoMo/Ti(20)-HMS sample is close to that of the oxide sample and implies that the sintering involves the Co species adsorbed on the Ti ions. The Co/Mo ratio of the samples also decreases in comparison with that of the freshly sulfided catalysts. This decrease is more pronounced for the two samples with Si/Ti = 40 and 20 (Table 4), due to the redispersion of Mo and the sintering of the Co species.

The ratio between the oxided and sulfided Co species decreases slightly in all used samples [with the CoMo/Ti(40)-HMS sample still having the highest value] except the high-Ti content sample, the value of which increases in comparison with that of the freshly sulfided catalyst. These results suggest that a very small part of the oxide Co species is sulfided during the reaction, and the excess sulfur is bound predominantly to the Mo species. The unexpected increase of the oxide species in the high-Ti content sample at the reductive conditions of the reaction could be explained by the specific sintering of Co in this sample, which results in surface enrichment of the particles with the oxide phase at the expense of the sulfided Co ions.

Finally, the BE values of Ti are preserved for all samples in the oxide, sulfided, and used catalysts, indicating that neither the sulfidation nor the reaction conditions cause changes in electronic properties. In general, the XPS results indicate that the evolution of the samples from the oxide state to the sulfided sample and used sample states is ratter complex, and the presence of Ti in the samples leads to a number of phenomena that generate a complex relation between dispersion/sintering, Co/Mo atomic ratio, degree of oxidation/sulfidation, and spe-

cific electronic properties of each sample that should be reflected in the catalytic activity performance in this dynamic system.

3.7. Catalytic activity and selectivity

The product distribution on the various catalysts is given in Table 5. The first samples for GC analysis were obtained after 50 min on stream for all catalysts. The values in brackets indicate the percentage of the corresponding compound after 4 h on stream. The product distribution of the Ti-free sample indicates that the reaction route on this sample proceeds probably via total dealkylation of the aromatic rings followed by hydrodesulfurization. No hydrogenated products are observed on this catalyst. Note that with the exception of the Ti-free sample, all other catalysts demonstrate partial and total dealkylation and isomerization ability due to the presence of the corresponding compounds. The amounts of these compounds are the highest in the sample with a Si/Ti = 40 molar ratio; however, their content decreases slightly in this sample after 4 h on stream, whereas for the other Ti-containing samples, the amount of partially dealkylated and isomerized products increases after 4 h on stream. This increase is more pronounced for the CoMo/Ti-(20)HMS sample, whereas for the industrial catalysts practically no change is observed.

Bi-phenyl (BP) is present in the product distribution of all catalysts. Its content is greatest on the industrial catalysts, followed by the catalyst with a Si/Ti = 40 molar ratio. The amount of BP decreases slightly on this catalysts after 4 h of reaction, whereas it increases at the end of the test on the samples with Si/Ti = 20 and 80 molar ratios.

DBT is present in the greatest amount on the industrial catalysts. It seems that this catalyst demonstrates the highest total dealkylation activity, but its desulfuration activity is impeded. The lowest DBT content is observed at the beginning of the tests on the sample with a Si/Ti = 20 molar ratio. However, the amount of unreacted 4E6MDBT is very high on this catalyst, which explains the low content of DBT in the product distribution. After 4 h on stream, the amount of DBT on this catalyst more than doubles, due to increased dealkylation of the reagent. The Ti-free catalyst shows the lowest DBT content after 4 h on stream due to deactivation. The catalyst with a Si/Ti = 40 molar ratio demonstrates a small decrease in the DBT content after 4 h on stream, probably due to some deactivation, because the amount of unprocessed 4E6MDBT after 4 h of work increases slightly, whereas the content of all other reaction products decreases slightly. The sample with a Si/Ti molar ratio = 80 shows a significant increase in DBT content after 4 h of work, whereas the 4E6MDBT content strongly decreases. Obviously, this catalyst's total and partial dealkylation ability increase over time, but its HDS ability does not increase proportionally in comparison to that at the beginning of the tests.

The product distribution indicates that the HDS on the Ti-containing catalysts proceeds via different routes and on different active sites, each making a different contribution to the final results. Obviously, as indicated by the presence of partially dealkylated and isomerized products, one route is the partial dealkylation and isomerization of the initial reagent, followed by hydrodesulfurization and hydrogenation. The relatively high DBT content in the product distribution over all catalysts indicates that the predominant route of the reaction is via total dealkylation of the initial reagent, followed by direct desulfurization and hydrogenation. We suggest the following tentative reaction scheme, without excluding the possibility that short-lived intermediates exist in this complex reaction (Scheme 1).

The catalytic activity (expressed as total conversion and total S removed at TOS = 0 and 4 h), the degree of deactivation, and the amount of coke deposited on the samples is also given in Table 5. The industrial catalyst shows the highest total conversion. Moreover, its activity remains practically constant. Next, according to its total conversion, is the catalyst with a Si/Ti = 40 ratio. However, this catalyst suffers slight deactivation with time on stream. The Ti-free catalyst shows the lowest total conversion. The catalysts with Si/Ti = 80 and 20 molar ra-

Table 5
Products distribution in the HDS of 4E6MDBT[a] over the industrial and CoMo/Ti(x)-HMS catalysts

Catalyst	Products distribution							Total S removed at TOS = 0 h (4 h) (%)	Coke[b] (%)
	Dealkylation route				Isomerization route		Unreacted 4E6MDBT (%)		
	DCH (%)	CHB (%)	BP (%)	DBT (%)	3,6-DMBF (%)	3,6-DMDCH (%)			
CoMo/HMS	0.00 (0.00)	0.00 (0.00)	3.64 (3.53)	8.76 (6.67)	0.00 (0.00)	0.00 (0.00)	83.70 (89.80)	4.14 (3.52)	0.9
CoMo/Ti(80)-HMS	0.34 (0.54)	1.50 (2.40)	6.58 (10.55)	9.79 (15.68)	1.88 (3.01)	1.01 (1.62)	78.90 (66.20)	11.38 (18.12)	6.3
CoMo/Ti(40)-HMS	2.02 (1.88)	3.06 (2.85)	11.59 (10.79)	9.26 (8.62)	5.99 (5.57)	2.89 (2.69)	65.20 (67.60)	25.51 (23.80)	3.6
CoMo/Ti(20)-HMS	0.85 (1.82)	1.22 (2.60)	4.41 (9.45)	3.92 (8.38)	2.05 (4.39)	1.05 (2.25)	86.50 (71.10)	9.57 (20.50)	7.1
Industrial	1.70 (1.71)	2.98 (3.00)	12.48 (12.58)	16.17 (16.30)	2.04 (2.05)	2.34 (2.36)	62.30 (62.00)	21.80 (21.69)	n.d.

[a] Reaction conditions were: $T = 598$ K, $P = 5.0$ MPa, WHSV = 46.4 h^{-1}, TOS = 4 h.
[b] As determined from TGA measurements.

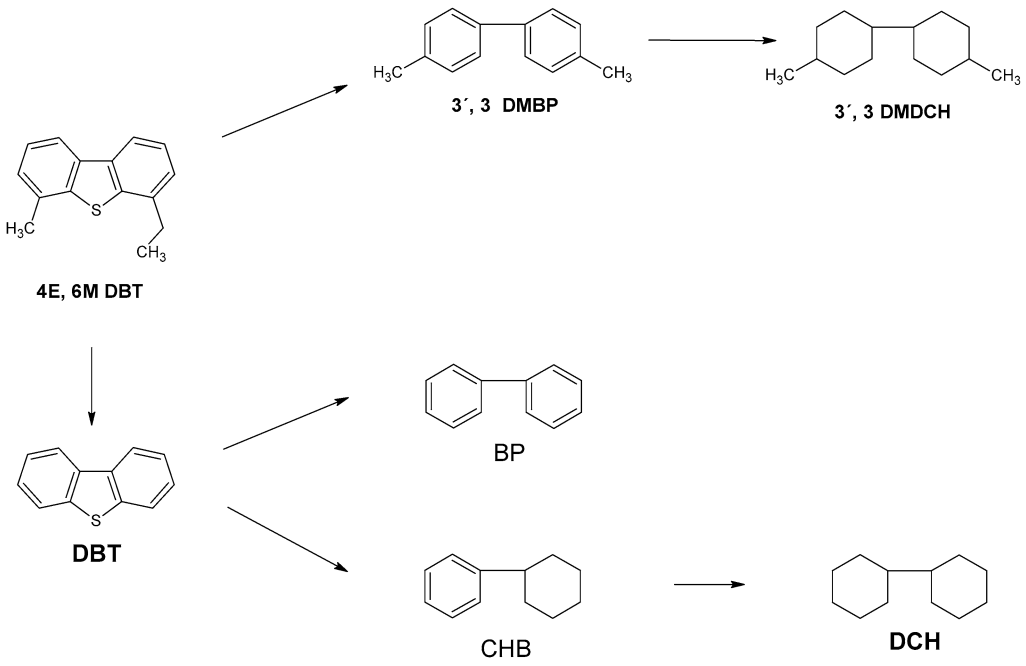

Scheme 1. Reaction scheme for the hydrodesulfurization of 4E6MDBT over the CoMo/Ti(x)-HMS catalysts.

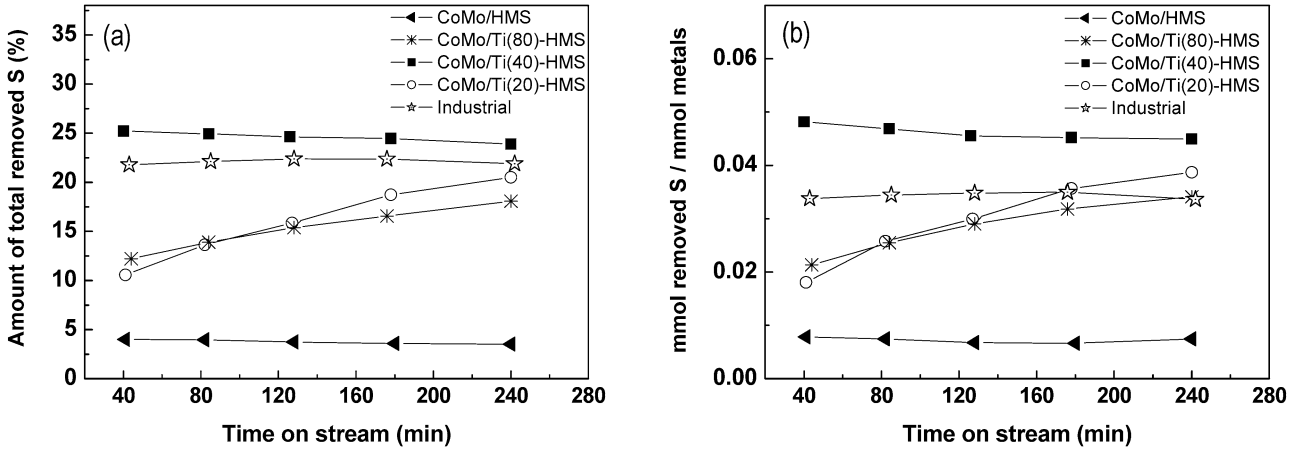

Fig. 8. Total amount of removed sulfur over CoMo/Ti(x)-HMS catalysts vs time on stream (a) and conversion expressed as the mmols of removed sulfur per mmol of metals vs time on stream (b).

tios differ from the other catalysts in that they have increased total conversion with time on stream. The catalyst with Si/Ti = 80 shows a slightly higher total conversion than the catalyst with Si/Ti = 40 after 4 h of reaction. However, the order of activity changes if we take into account that the total amount of removed sulfur is the aim of this reaction. Fig. 8a shows the total amount of removed sulfur versus time on stream. Now the sample with Si/Ti = 40 ratio is the most active catalysts, followed by the industrial catalyst. As in the case of total conversion, the other Ti-containing catalysts remove more sulfur with increasing time on stream. However, the sample with Si/Ti = 20 is more active than the sample with Si/Ti = 80 with respect to the total amount of sulfur removed. It seems that these two catalysts undergo certain changes in structure with time that might be related to the formation of new or more active sites under the conditions of the reaction.

Obviously, the activity depends strongly on the metal loading. The industrial catalyst (14.2 wt% Mo and 3.8 wt% Co) has a considerably higher metal content than our catalysts. A relatively justified comparison between the specific activities of the samples can be obtained by the amount of removed sulfur per mmol of metals (Co + Mo). Fig. 8b shows the mmols of removed sulfur per mmol of metals versus time on stream. Now the higher activity of the sample with Si/Ti = 40 is even more pronounced compared with the industrial catalysts. At the beginning of the test, this sample removes 42% more sulfur per mmol of metal content than the industrial one. After 4 h of work, its activity is 34% higher due to some deactivation of the catalyst. Both this sample and the industrial catalysts suffer deactivation versus time on stream (6.5 and 0.9%, respectively). Note that at the end of the tests, the activity of the other two Ti-containing samples increases and is higher than that of the

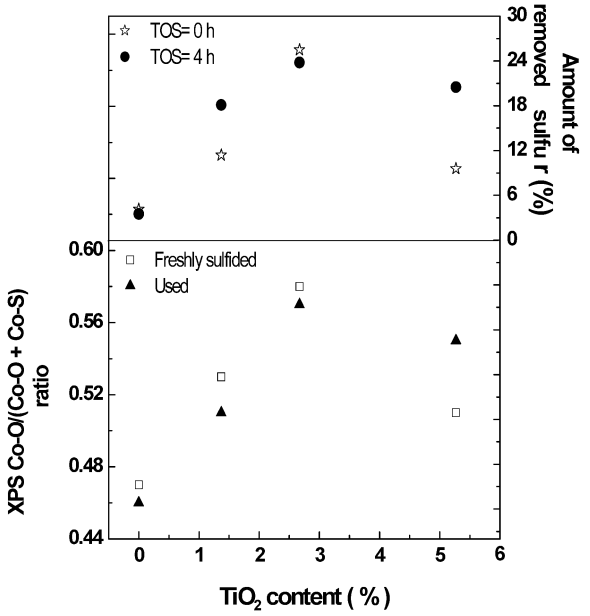

Fig. 9. Amount of the Co oxide species as determined by XPS (Table 4) vs the Ti content in the freshly sulfided and used catalysts and the amount of removed sulfur vs the Ti content at TOS = 0 and 4 h.

industrial catalysts. Obviously, these two samples do not suffer any deactivation at this stage of the reaction. The deactivation mechanisms are rather complex and differ in nature. Due to the presence of total or partial dealkylation reactions, accompanied by isomerization, one could suggest that the deactivation is caused by deposition of coke. Indeed, our preliminary DTA results (curves not shown here) indicate that coke is deposited on our catalysts. Surprisingly, the amount of this deposition is the highest on the two samples that do not manifest any deactivation. Obviously, the deactivation is caused not just by the presence of coke. The mechanism of deactivation should be studied in detail to gain better insight into its nature.

Although the HDS reaction of 4E6MDBT is rather complex and involves a number of reactions, we have observed certain relationships between Ti content, structural and electronic properties, and catalytic activity and selectivity of the samples. Fig. 9 shows the relationships between the amount of oxide/sulfided cobalt species (left axis) of the freshly sulfided and used catalysts and the amount of removed sulfur (right axis) at TOS (0 and 4 h) versus the Ti content. It is interesting that both types of curves follow exactly the same trend. Note that at the beginning of the reaction, the CoMo/Ti(80)-HMS catalyst removes slightly more sulfur than the CoMo/Ti(20)-HMS one. However, after 4 h of on-stream operation, due to changes occurring in the catalysts, as registered by the XPS measurements, the CoMo/Ti(20)-HMS sample has a greater amount of oxide species than the CoMo/Ti(80)-HMS sample and removes more sulfur than the CoMo/Ti(80)-HMS sample. Obviously, one of the most important effects of the Ti concentration is related to the sulfidability of the Co species, which varies in the different Ti-containing samples. It may be that the presence of different amounts of oxide Co species has an important effect on the dissociative adsorption of H_2 and hence on the acidity of the catalysts. As a result, the dealkylation and isomerization activity of the catalysts changes.

In general, it can be concluded that the HDS of 4E6MDBT proceeds via the initial dealkylization/isomerization reactions of the side chains, and the activity in these reactions correlates with the amount of oxide Co species. Once the steric hindrance of the alkyl chains is removed, the HDS reaction proceeds via the direct hydrodesulfurization and/or hydrogenation routes.

4. Discussion

The results of this study indicate that adding Ti to the HMS support increases the catalytic activity of the samples in the reaction of the HDS of 4E6MDBT. The effect of the Ti concentration is not linear, and the highest amount of removed sulfur is observed on the sample with Si/Ti ratio of 40. All characterization results indicate a strong electronic affect of the presence of Ti on the physicochemical properties of the samples and on their catalytic performance. We discuss some of the effects of Ti, which, in our opinion, can explain the catalytic activity in this complex reaction.

The structural parameters of the Ti-containing catalysts indicate that the catalytically active species are deposited predominantly on the outer surface of the supports, whereas for the Ti-free sample the deposition, as indicated by the decrease in pore diameter, also occurs in the pores of the HMS support. This unexpected result can be explained by the specific changes in the reactivity of the surface OH groups caused by the presence of Ti. Therefore, it can be suggested that the diffusion effects are avoided in the Ti-containing samples.

The presence of the Ti ions has a strong effect on the dispersion of the MoS_2 and Co species. Obviously, changes in the number of Mo ions in the corners and the edges of the particles should be expected, which is reflected in the catalytic behavior of the samples. This is also valid for the Co species. In addition, the Co/Mo ratio also changes with Ti concentration. The highest Co/Mo ratio is observed for the sample with Si/Ti = 40.

The presence of varying amounts of Ti in the samples changes not only the amount of single silanol groups, but also the reactivity (a purely electronic effect) of these groups, as well as the reactivity of the OH groups bound to Ti. The ^{1}H-NMR spectra indicate that very few Ti–OH groups are involved in the deposition of the active species in the sample with the highest Ti content, whereas the peak almost disappears for the other Ti-containing samples. The Ti/Si atomic ratio (Table 4) indicates that the evolution of the samples is very dynamic. The Ti/Si values of the pure supports increase with increasing Ti concentration. This also holds for the catalysts in their oxidized state. However, the Ti/Si values in the oxidized state of the catalysts are much higher than those in the pure supports. The sulfidation of the samples results in a drastic decrease in Ti/Si values in comparison to the oxidized samples. The reaction conditions (after 4 h on stream) lead to an increase in the values of the Ti/Si atomic ratio for all samples. The changes of the Ti/Si values cannot be explained simply by the redispersion/sintering processes observed for the active species. Migration of Ti ions to the surface and even some segregation of TiO_2 likely occur

during the reaction. It is obvious that whatever the origin of this behavior, direct contact between the active species and the Ti ions would result in changes in the interaction with the support and hence in their electronic properties, which should be reflected in the catalytic performance of the samples.

The catalytic activity results indicate that the HDS reaction of 4E6MDBT proceeds via the initial total or partial dealkylation and isomerization of the reagent. Both reactions need acid sites. The acidity results of the sulfided samples indicate that in the presence of Ti, both the L and B sites increase. The effect of Ti concentration is not linear, with the highest acidity observed on the Si/Ti = 40 sample. Once the steric hindrance of the side chain is removed, adsorption of the modified initial reagent on the HDS sites is possible and direct HDS occurs. Note that the NO adsorption results indicate that the Si/Ti = 40 sample contains the greatest amount of surface exposed Mo and Co species on which the DDS takes place. An important question arises as to why this sample has the highest acidity. Is this acidity related to easier heterolytic dissociation of H_2? If so, is the heterolytic dissociation related just to the higher number of surface exposed Mo and Co species or also to their specific electronic properties? The XPS and the NO adsorption results indicate that a significant portion of the Co ions is not sulfided at the sulfidation conditions applied in this study. The greatest amount of oxidized Co species is observed in the Si/Ti = 40 sample. Little or no attention has been given to the oxidized species of the promoter, although their presence is well known. The correlation observed between the amount of oxidized Co species and the acidity of the samples on one hand and the amount of removed sulfur on the other hand leads us to suggest that the presence of these species plays a role in the dissociation of H_2 molecules. Indeed, the Co ions in the oxidized species are more positively charged than those in the sulfided species and could more easily dissociate the H_2 molecule. If this were true, then the highest acidity and catalytic activity of the Si/Ti = 40 sample should be related to the easier dissociation of the H_2 molecules in the presence of oxidized Co species. The sensitivity of a sample's catalytic performance to the amount of oxidized Co species present is supported by the fact that after 4 h on stream, the Si/Ti = 20 sample removes more sulfur than the Si/Ti = 80 sample due to the higher amount of oxidized species in the former (Table 4).

Additional studies are needed to clarify the effect of the oxidized Co species on the dissociation of H_2 and on the electronic properties of supported species. In any case, just the presence of these oxidized species and their contact with the sulfided Co and Mo ions should lead to changes in the electronic properties of the sulfided species.

Some important questions arise. Where are the oxidized cobalt ions situated? Do they participate in the so-called "Co-MoS" phase? Are they situated on the surface of semi-sulfided cobalt particles or a part of the cobalt particles, due to their size and particular interaction with the support remain in a completely oxidized form and contribute to the band of the adsorbed NO on oxidized cobalt species? We cannot give unambiguous answers to these questions. Further studies are needed to investigate the effects of these oxidized species on catalytic activity. The answers to these questions could provide additional insight into the active site(s) and mechanisms of the HDS reactions.

In conclusion, we can deduce from our results that the presence of Ti leads to multiple nonlinear effects on the structure, chemical composition, and specific electronic properties of the active species.

5. Conclusion

The effect of the presence of varying Ti concentrations introduced into hexagonal mesoporous silica (HMS) support on the catalytic activity of CoMo/Ti(x)-HMS catalysts was evaluated in the HDS of 4E6MDBT. The highest HDS activity was observed on the catalyst with a Si/Ti molar ratio of 40. The HDS of 4E6MDBT over the Ti-containing catalysts proceeds via total or partial DA and is accompanied by isomerization of the side chains. Then DDS and hydrogenation (HYD) reactions occur. The HDS of 4E6MDBT in the Ti-free catalyst proceeds via DA and DDS pathways (4E6MDBT→DBT → BF). During the reaction, additional redispersion of the molybdenum species is observed, whereas in the two samples with the highest Ti content, sintering of the cobalt species occurs. A correlation between the amount of oxide Co species of the freshly sulfided and used catalysts and the HDS activity of the samples was noted.

Acknowledgments

The authors thank Professors P.L. Arias and J.F. Cambra, University of the Basque Country (School of Engineering) for providing the 4E6MDBT. T.A. Zepeda is grateful to ICP-CSIC Spain and CONACyT México for financial support. The financial support of DGAPA, UNAM, México, is gratefully acknowledged. The Spanish Ministry of Science and Technology is also acknowledged for funding the PPQ2002-11841-E project.

References

[1] B.C. Gates, J.R. Katzer, G.C.A. Schuit, Chemistry of Catalytic Processes, McGraw–Hill, New York, 1979, p. 390.
[2] G.C.A. Schuit, B.C. Gates, AIChE J. 19 (1973) 417.
[3] H. Topsøe, B.S. Clausen, F.E. Massoth, in: J.R. Anderson, M. Boudard (Eds.), Catalysis-Science and Technology, vol. 11, Springer, Berlin, 1996.
[4] C. Song, C.S. Hsu, I. Mochida, Chemistry of Diesel Fuels, in: Applied Energy and Technology Series, Taylor & Francis, London, 2000.
[5] K.G. Knudsen, B.H. Cooper, H. Topsøe, Appl. Catal. A Gen. 189 (1999) 205.
[6] C. Song, Catal. Today 86 (2003) 211.
[7] I.V. Babich, J.A. Moulijn, Fuel 82 (2003) 607.
[8] X.L. Ma, K. Sakanishi, I. Mochida, Ind. Eng. Chem. Res. 35 (1996) 2487.
[9] W.R.A.M. Robinson, J.A.R. van Veen, V.H.J. de Beer, R.A. van Santen, Fuel Proc. Technol. 61 (1999) 89.
[10] W.R.A.M. Robinson, J.A.R. van Veen, V.H.J. de Beer, R.A. van Santen, Fuel Proc. Technol. 61 (1999) 103.
[11] T. Kabe, A. Ishihara, H. Tajima, Ind. Eng. Chem. Res. 31 (1992) 1577.
[12] F. Bataille, J.L. Lemberton, P. Michaud, G. Perot, M. Vrinat, M. Lemaire, E. Schulz, M. Breysse, S. Kasztelan, J. Catal. 191 (2000) 409.
[13] D.D. Whitehurst, T. Isoda, I. Mochida, Adv. Catal. 42 (1998) 345.
[14] M.V. Landau, D. Berger, M. Herskowitz, J. Catal. 159 (1996) 236.

[15] T. Isoda, X. Ma, I. Mochida, Preprints 39 (1994) 584.
[16] C. Kwak, Mi Young Kim, K. Choi, S. Heup Moon, Appl. Catal. A Gen. 185 (1) (1999) 19.
[17] T. Isoda, S. Nagao, X. Ma, Y. Korai, I. Mochida, Energy Fuels 10 (1996) 1078.
[18] T.A. Zepeda, J.L.G. Fierro, B. Pawelec, R. Nava, T. Klimova, G.A. Fuentes, T. Halachev, Chem. Mater. 17 (2005) 4062.
[19] E.J.M. Hensen, V.H.J. de Beer, J.A.R. van Veen, R.A. van Santen, J. Catal. 215 (2) (2003) 353.
[20] P.T. Tanev, T. Pinnavaia, Science 267 (1995) 865.
[21] P. Tanev, M. Chibwe, T.J. Pinnavaia, Nature 368 (1994) 321.
[22] S. Gotier, A. Tuel, Zeolites 15 (1995) 601.
[23] C.T. Kresge, M.E. Leonowich, W.J. Roth, J.C. Vartuli, J.S. Beck, Nature 359 (1992) 710.
[24] B. Pawelec, S. Damyanova, R. Mariscal, J.L.G. Fierro, I. Sobrados, J. Sanz, L. Petrov, J. Catal. 223 (1) (2004) 86.
[25] T. Armaroli, Top. Catal. 15 (2001) 63.
[26] S. Damyanova, L. Dimitrov, R. Mariscal, J.L.G. Fierro, L. Petrov, I. Sobrados, Appl. Catal. A Gen. 256 (2003) 183.
[27] S. Razi Seyedmonir, S. Abdo, R.F. Howe, J. Phys. Chem. 86 (1982) 1233.
[28] P. Schacht, L. Noreña-Franco, J. Ancheyta, S. Ramírez, I. Hernández-Pérez, L.A. García, Catal. Today 98 (2004) 115.
[29] V.M. Mastikhin, I.L. Mudrakovski, A.V. Nosov, Prog. NMR Spectrosc. 23 (1991) 259.
[30] N.Y. Topsøe, H. Topsøe, J. Catal. 84 (1983) 386.
[31] J. Ramirez, R. Cuevas, A. Lopez Agudo, J.L.G. Fierro, Appl. Catal. 57 (1990) 223.
[32] K. Kabe, A. Ishihara, W. Qian, Hydrodesulfurization and Hydrodenitrogenation, Kodansha, Tokyo, 1999.
[33] M. Yamada, T. Obara, J. Jpn. Pet. Inst. 33 (4) (1990) 221.
[34] H. Topsøe, B.S. Clausen, N. Topsøe, E. Pederson, Ind. Eng. Chem. Fundam. 25 (1986) 25.
[35] R. Prada Silvy, J.L.G. Fierro, P. Grange, B. Delmon, in: B. Delmon, P. Grange, P.A. Jacobs, G. Poncelet (Eds.), Preparation of Catalysis, vol. IV, Elsevier, Amsterdam, 1987, p. 605.
[36] X. Wang, U.S. Ozkan, J. Phys. Chem. B 109 (2005) 1882.
[37] X. Wang, U.S. Ozkan, J. Mol. Catal. A 232 (2005) 101.
[38] J.W. Ward, in: J.A. Rabo (Ed.), Zeolite Chemistry and Catalysis, in: ACS Monograph, vol. 171, Am. Chem. Soc., Washington, DC, 1976, p. 118.
[39] D. Briggs, M.P. Seah (Eds.), Practical Surface Analysis by Auger and X-Ray Photoelectron Spectroscopy, Wiley, New York, 1990, p. 607.
[40] V.I. Nefedov, M.N. Firsov, I.S. Shaplygin, J. Electron Spectrosc. Relat. Phenom. 26 (1982) 65.
[41] P. Arnoldy, M.C. Franken, B. Scheffer, J.A. Moulijn, J. Catal. 96 (1985) 381.
[42] R.I. Declerck-Grimee, P. Canesson, R.M. Friedman, J.J. Fripiat, J. Phys. Chem. 82 (8) (1978) 889.
[43] H. Shimada, Catal. Today 86 (2003) 17.